Tribology and Materials
Vol. 5, No. 2, 2026, pp. 50-62
ISSN 2812-9717
https://doi.org/10.46793/tribomat.2026.004

Optimisation of microstructure and wear properties of porous Fe-Cu bearing materials

Sutrisna SUTRISNA [1,*], Muhamad Jalu PURNOMO [2], Wartono WARTONO [1], Angger Bagus PRASETIYO [3], Mohammad Imami Syacitta RIADJI [1], Waldi Putra MINGWARO [1]

[1] Faculty of Engineering and Planning, Institut Teknologi Nasional Yogyakarta, Yogyakarta, Indonesia
[2] Faculty of Aerospace Technology, Institut Teknologi Dirgantara Adisutjipto, Yogyakarta, Indonesia
[3] Faculty of Engineering, Universitas Tidar, Magelang, Indonesia
*Corresponding author: sutrisna@itny.ac.id

Keywords
Fe-Cu alloy
mechanical alloying
porous bearing
wear resistance
sintering

History
Received: 13-10-2025
Revised: 06-12-2025
Accepted: 24-12-2025

Abstract

Optimising Fe-Cu porous bearing materials is essential for improving durability and wear resistance in automotive systems. However, the combined influence of mechanical alloying and sintering processes on their microstructural properties and tribological response has not been systematically clarified. In this study, a Fe-20Cu alloy was fabricated via mechanical alloying for 4, 8, 12 and 16 h, followed by sintering at 800, 900 and 1000 °C. X-ray diffraction revealed progressive peak broadening and structural refinement with increasing milling time, while scanning electron microscopy indicated a transformation from coarse, heterogeneous particles (4 h) to refined, compact structures after extended milling. Sintering improved interparticle bonding and densification, with the most uniform and consolidated microstructure obtained at 1000 °C. Energy-dispersive X-ray mapping confirmed enhanced Fe-Cu mixing with minor oxide enrichment. Testing demonstrated the lowest wear rate (1.45×10^{-4} mm^3/m) and the highest density (7.22 g/cm^3) for the sample obtained after 12 h of milling and sintering at 1000 °C. Excessive milling (16 h) slightly lowered densification due to particle reagglomeration. Overall, 12 h of milling combined with sintering at 1000 °C provides the optimal balance between densification, microstructural refinement and wear resistance, confirming Fe-Cu porous alloys as promising candidates for high-performance applications.

1. Introduction

Porous bearings are widely utilised in automotive and industrial systems owing to their inherent ability to provide self-lubrication, reduced friction and reliable performance under diverse load conditions. Among the various compositions explored, Fe-Cu based alloys have received particular attention because they combine the mechanical strength of Fe with the thermal and electrical conductivity of Cu [1], rendering them suitable for dynamic vehicle components such as bearings [2-4]. Despite these advantages, optimising the microstructure and tribological behaviour of Fe-Cu porous bearings remains challenging, particularly in achieving the delicate balance between density, wear resistance and porosity that governs their long-term functional reliability [5,6].

Mechanical alloying has emerged as an effective processing route in powder metallurgy for refining microstructure, improving phase homogeneity and tailoring material properties. Extended milling enhances solid-state mixing between Fe and Cu while increasing defect density and stored strain energy, which influence hardness and wear resistance [7-10]. Prior studies have shown that prolonged milling can reduce grain size and improve densification during sintering. However, excessive milling may also cause particle agglomeration and

retain residual porosity, thereby compromising density and mechanical integrity [11]. This indicates that there is still no clear consensus on the optimum milling time that ensures both high densification and superior wear performance.

Similarly, sintering temperature plays a decisive role in determining the final properties of Fe-Cu bearings. Lower sintering temperatures generally lead to incomplete particle bonding, whereas higher temperatures (≥ 1000 °C) improve densification but may induce grain coarsening or undesirable phase evolution [12-14]. While several studies have independently investigated the effects of milling or sintering, comparatively few have systematically examined the combined influence of both parameters on the processing-structure-property relationship of Fe-Cu porous bearing materials. This lack of integrated optimisation represents a key research gap that limits the development of bearings capable of meeting the stringent demands of high-performance systems [15,16].

In this study, although prior work has separately explored mechanical alloying and sintering for the Fu-Cu system, limited research has mapped the combined effects of milling time and sintering temperature on porous Fe-20Cu bearing material for automotive applications [17]. The present work addresses this gap by quantifying densification, phase evolution, Cu distribution and tribological response across a matrix of milling times (4, 8, 12 and 16 h) and sintering temperatures (800, 900 and 1000 °C). Structural evolution was characterised by X-ray diffraction (XRD), while scanning electron microscopy (SEM) and energy-dispersive X-ray spectroscopy (EDS) were used to assess morphological features and elemental distribution. In addition, density measurements and wear tests were conducted to evaluate functional performance. By systematically correlating milling time and sintering temperature with microstructure, density and wear resistance, this study aims to identify the optimum processing parameters. The findings clarify the processing-structure-property relationship in Fe-Cu porous alloys and advance their potential as reliable candidates for high-performance applications.

2. Materials and methods

High-purity elemental powders of iron (Fe, ≥ 99.5 %, < 45 μm) and copper (Cu, ≥ 99.7 %, < 50 μm) were selected as the starting materials. A nominal composition of 80 wt. % Fe and 20 wt. % Cu (Fe-20Cu) was chosen because this alloy is widely used in porous bearings due to its balance of mechanical strength and self-lubricating capability.

Mechanical alloying was performed in a high-energy planetary ball mill using stainless steel vials and 10 mm diameter balls at a ball-to-powder weight ratio of 10 : 1. Milling was conducted at 300 rpm under a protective argon atmosphere to minimise oxidation. The milling times were varied (4, 8, 12 and 16 h) to investigate the influence of processing time on phase evolution and microstructure development. To prevent excessive heating, milling was carried out in cycles of 30 min operation followed by 10 min rest.

The milled powders were uniaxially cold die-pressed into cylindrical compacts at 500 MPa using a hardened steel die. The cylindrical compacts had dimensions of 10 mm in diameter and 5 mm in height. Sintering was performed in a tube furnace under flowing argon at three temperatures (800, 900 and 1000 °C), with a heating rate of approximately 10 °C/min, a cooling rate of approximately 5 °C/min and a soaking time of 2 h. The atmosphere was intended to suppress oxidation and promote solid-state diffusion between Fe and Cu particles.

Phase analysis was conducted by X-ray diffraction (XRD) using Cu Kα radiation (λ = 1.5406 Å) over the 2θ range of 20 – 80° with a step size of 0.02°. Microstructural features of the powders and sintered compacts were examined using JEOL JSM-7000 scanning electron microscopy (SEM) equipped with an energy-dispersive X-ray spectroscopy (EDS) detector for elemental mapping. These characterisations were used to correlate milling time and sintering temperature with particle refinement, densification and phase distribution.

The bulk density of the sintered samples was measured using the Archimedes method with distilled water as the immersion medium.

Tribological performance was evaluated using a pin-on-ring tribometer under dry sliding conditions, with a normal load of 62.37 N, a sliding speed of 0.1 m/s and a sliding distance of 15 m, at room temperature. The pin was a tested sample (cylindrical compact with a diameter of 10 mm and a height of 5 mm), and the counter-body (ring with a thickness of 3.45 mm and a radius of 13.6 mm) was made of hardened steel AISI 52100, with a hardness of 60 – 62 HRC [18]. Wear tests produced a wear scar of variable width and 3.45 mm in length on the pin surface.

The wear scar width was measured using an Olympus SZ-PT stereo zoom microscope at 40× magnification. Considering the applied magnification, the effective measurement resolution was approximately 0.025 mm. For each specimen, the used wear scar width represents the average of measurements taken at multiple locations along the wear track. The wear rate was calculated from the measured wear volume divided by the sliding distance. For accuracy, at least three tests were performed for each sample, and then the average was taken.

3. Results and discussion

3.1 Structural changes with milling time

Figure 1 presents the XRD patterns of Fe-20Cu powder milled for 4, 8, 12 and 16 h and subsequently sintered at 1000 °C (Fig. 2). The evolution of the diffraction peaks reflects the combined effects of mechanical alloying and thermal consolidation on crystallinity, phase distribution and defect structure [19].

After 4 h of milling, the α-Fe (BCC) and Cu (FCC) peaks appear sharp and well-defined, accompanied by noticeable Fe_2O_3 reflections, indicating coarse crystallites, incomplete intermixing and residual oxide contamination from the starting powders [20]. After 8 h of milling, peak broadening becomes evident together with a reduction in oxide intensity, signifying increased lattice strain and enhanced Fe-20Cu powder homogenisation through repeated cold welding and fracturing.

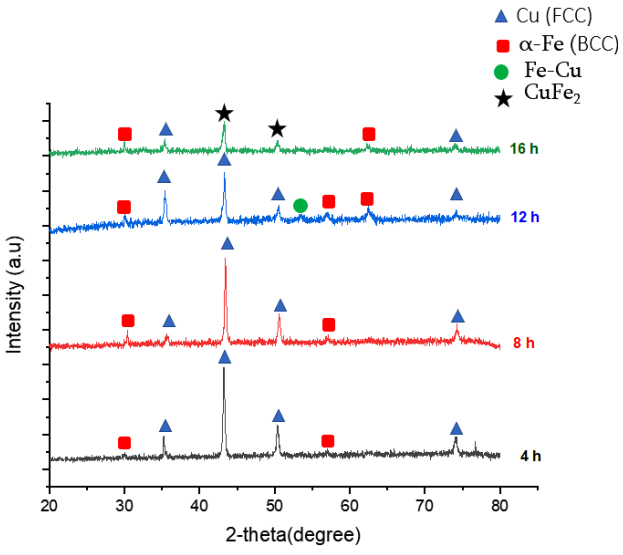

Figure 1. XRD patterns of Fe-20Cu powder milled for 4, 8, 12 and 16 h

A more pronounced structural refinement occurs after 12 h, where α-Fe and Cu peaks narrow and oxide signatures diminish further. This indicates improved defect recovery and more efficient solid-state diffusion during sintering. In contrast, extending the milling time to 16 h produces only a marginal improvement. Instead, the re-emergence of peak broadening suggests excessive strain accumulation and localised reagglomeration, which limit additional crystallite refinement.

Sintering promotes further structural development, especially for longer milling times (Fig. 2). Oxide-related features (Fe_2O_3) remain visible in the 4 h condition but are significantly weakened in the samples milled for 8 and 12 h and sintered at 1000 °C. The sample milled for 12 h and sintered exhibits the clearest α-Fe and Cu peaks with minimal oxide signals, reflecting optimal homogenisation prior to sintering [21]. Although the sample milled for 16 h and sintered retains a refined structure, its broader peaks indicate residual strain that is not fully relieved during sintering.

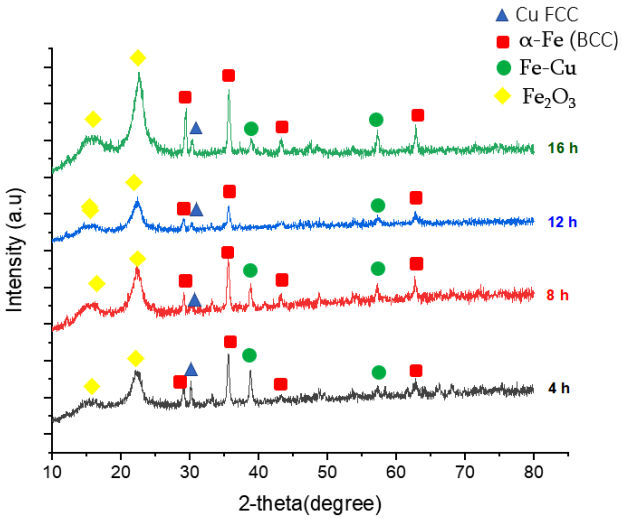

Figure 2. XRD patterns of Fe-20Cu alloy milled for 4, 8, 12 and 16 h and sintered at 1000 °C

The Cu-Fe intermetallic phases (such as $CuFe_2$) were not detected under any condition, which is consistent with the immiscibility of the Fe-Cu system within the investigated thermal range. Overall, the XRD results show that mechanical alloying enhances powder mixing and crystallite refinement up to an optimum of approximately 12 h mixing time, providing the most favourable structural state for subsequent densification during sintering [22].

3.2 Morphological changes with milling time

Figure 3 presents SEM micrographs of the Fe-20Cu alloy powders after different milling times

and sintered at 1000 °C. The morphological evolution clearly illustrates the competing effects of cold welding and fracturing that govern mechanical alloying, leading to progressive refinement and improved mixing of the constituents. After 4 h of milling, the powders exhibit relatively coarse, irregular polyhedral morphologies with large flat surfaces and distinct particle boundaries.

After 8 h of milling, the particles exhibit more pronounced fragmentation, with clear fracture surfaces and a noticeable reduction in average particle size. The powders now consist of a mixture of flattened lamellae and finer debris, reflecting the competitive interaction between cold welding and fracturing typical of intermediate milling stages [23]. The presence of smaller particles

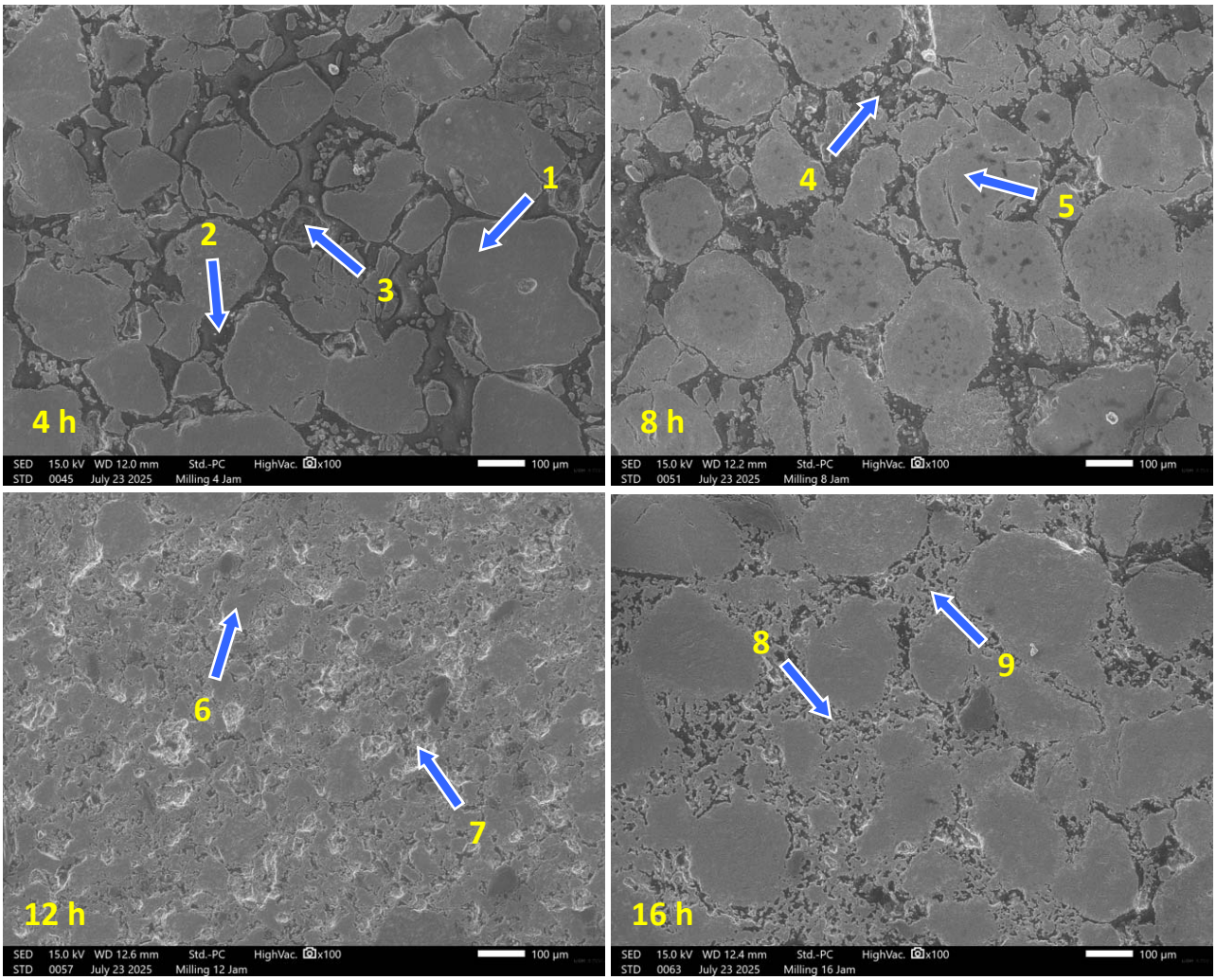

Figure 3. SEM images of the Fe-20Cu alloy milled for 4, 8, 12 and 16 h and sintered at 1000 °C; EDS points are denoted with arrows

Table 1. EDS analysis (wt. %) of the Fe-20Cu alloy in points denoted in Figure 3

Element	Fe	Cu	Mg	Al	Si	Ti	C	O
Point 1	55.08	–	1.16	1.91	0.17	3.93	16.55	21.19
Point 2	1.86	13.62	0.01	–	–	0.36	72.59	11.55
Point 3	8.46	5.10	–	9.61	–	1.20	51.74	23.89
Point 4	0.60	9.73	–	1.05	0.19	0.03	72.71	15.68
Point 5	56.64	–	0.56	1.00	0.04	6.74	7.44	27.57
Point 6	49.68	6.45	0.80	0.96	–	7.73	7.89	26.47
Point 7	1.93	2.82	4.69	0.22	0.30	0.42	37.04	52.59
Point 8	29.85	9.32	–	3.98	–	2.83	33.71	20.31
Point 9	14.58	9.43	–	2.61	3.54	1.47	44.52	23.86

dispersed within larger agglomerates indicates greater refinement and enhanced intermixing between Fe and Cu, indicating the onset of more effective solid-state mixing.

At 12 h of milling, the microstructure becomes significantly refined and homogeneous. The distinction between Fe-rich and Cu-rich particles becomes less pronounced, and the morphology transitions toward irregular but more uniformly sized particles. This refinement correlates with the narrowing and increased intensity of XRD peaks (Fig. 1), suggesting enhanced solid-state mixing and improved structural uniformity. The reduced presence of large flat surfaces and the dominance of smaller, equiaxed particles imply that fracturing increasingly outweighs cold welding at this stage.

In contrast, the powders milled for 16 h exhibit a more agglomerated microstructure. Although fine, irregular particles are still present, localised cold welding leads to the formation of larger aggregates. The prolonged milling energy at this stage promotes particle agglomeration and strain hardening, partially counteracting the earlier refinement. This morphological coarsening aligns with the XRD results (Fig. 1), where broader peaks and slightly reduced intensity suggest increased lattice strain and defect accumulation rather than continued refinement.

The EDS results (Table 1) indicate that Fe is the dominant constituent in most analysed locations, with contents generally ranging from 55 to 57 wt. %, while Cu is the second major element with approximately 13 – 15 wt. %. A local deviation is observed at point 6, where the Fe content decreases to 50 wt. %, reflecting compositional heterogeneity within the sintered microstructure. The additional elements Mg, Al, Si and Ti occur with several wt. %, indicating that they are not merely trace species. This elemental distribution is consistent with the nominal Fe-20Cu alloy composition and suggests that the minor constituents, likely introduced from the starting powders or milling media, contribute to the presence of multiple solute species that can influence grain-boundary chemistry and promote secondary-phase formation [24]. The nonhomogeneous Cu distribution indicates that the Cu phase has not yet been uniformly incorporated into the Fe matrix. The surface morphology, dominated by flat and angular particles, suggests that cold welding is the prevailing mechanism at this early stage, resulting in limited refinement, which is consistent with the broad, low-intensity XRD peaks (Fig. 1) that reflect poor crystallinity.

3.3 Morphological changes with sintering temperature

Microstructural changes with sintering temperature are shown only for the samples milled for 16 h (Fig. 4). This condition was chosen because it exhibits the most pronounced changes in phase distribution and grain coarsening, thereby providing a clearer representation of how sintering

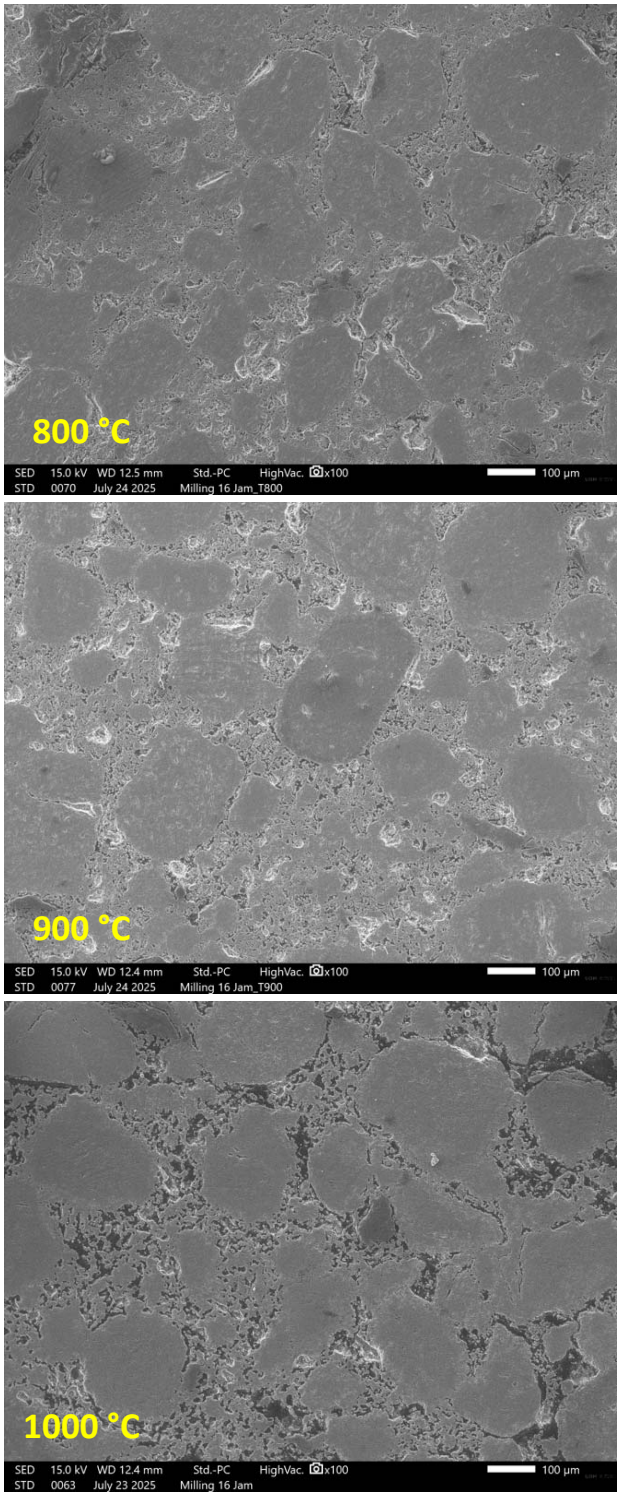

Figure 4. SEM images of the Fe-20Cu alloy milled for 16 h and sintered at 800, 900 and 1000 °C

temperature affects Fe-Cu segregation, oxide development and pore closure compared with samples milled for shorter times [25].

At a sintering temperature of 800 °C, prolonged milling promotes enhanced Fe-Cu phase intermixing and a reduction in compositional heterogeneity, as reflected in the SEM micrographs and supported by density-derived consolidation behaviour. The Fe-20Cu alloy exhibits a relatively homogeneous phase distribution accompanied by comparatively smaller grain sizes. The elemental distribution of Fe, Cu, O and minor alloying elements for the sample milled for 16 h and sintered at 800 °C is illustrated by the EDS mapping analysis (Fig. 5). However, the presence of residual surface porosity indicates incomplete structural homogenisation, suggesting that diffusion and solid-state reactions are not yet fully achieved at this temperature. Despite this limitation, the material maintains adequate structural integrity, although further thermal exposure could enhance atomic mobility and improve consolidation [26].

When sintered at 900 °C, the microstructure reveals a more distinct distribution of Fe- and Cu-rich regions compared to the 800 °C condition. The redistribution of Fe- and Cu-rich regions together with grain-boundary segregation of oxygen and minor elements at 900 °C is clearly shown in the EDS maps presented in Figure 6. Grain coarsening becomes more pronounced, while overall porosity decreases, implying that sintering at this temperature effectively promotes densification and healing of microstructural defects. This condition manifests as microstructural degradation, as defect annihilation enhances cohesion without excessive grain growth.

At a sintering temperature of 1000 °C, pronounced Cu segregation and oxygen accumulation along grain boundaries are evident, as confirmed by the EDS mapping analysis (Fig. 7). Pronounced grain coarsening is also noticed, driven by intensified atomic diffusion and grain boundary migration. This high-temperature treatment promotes densification and a clearer phase

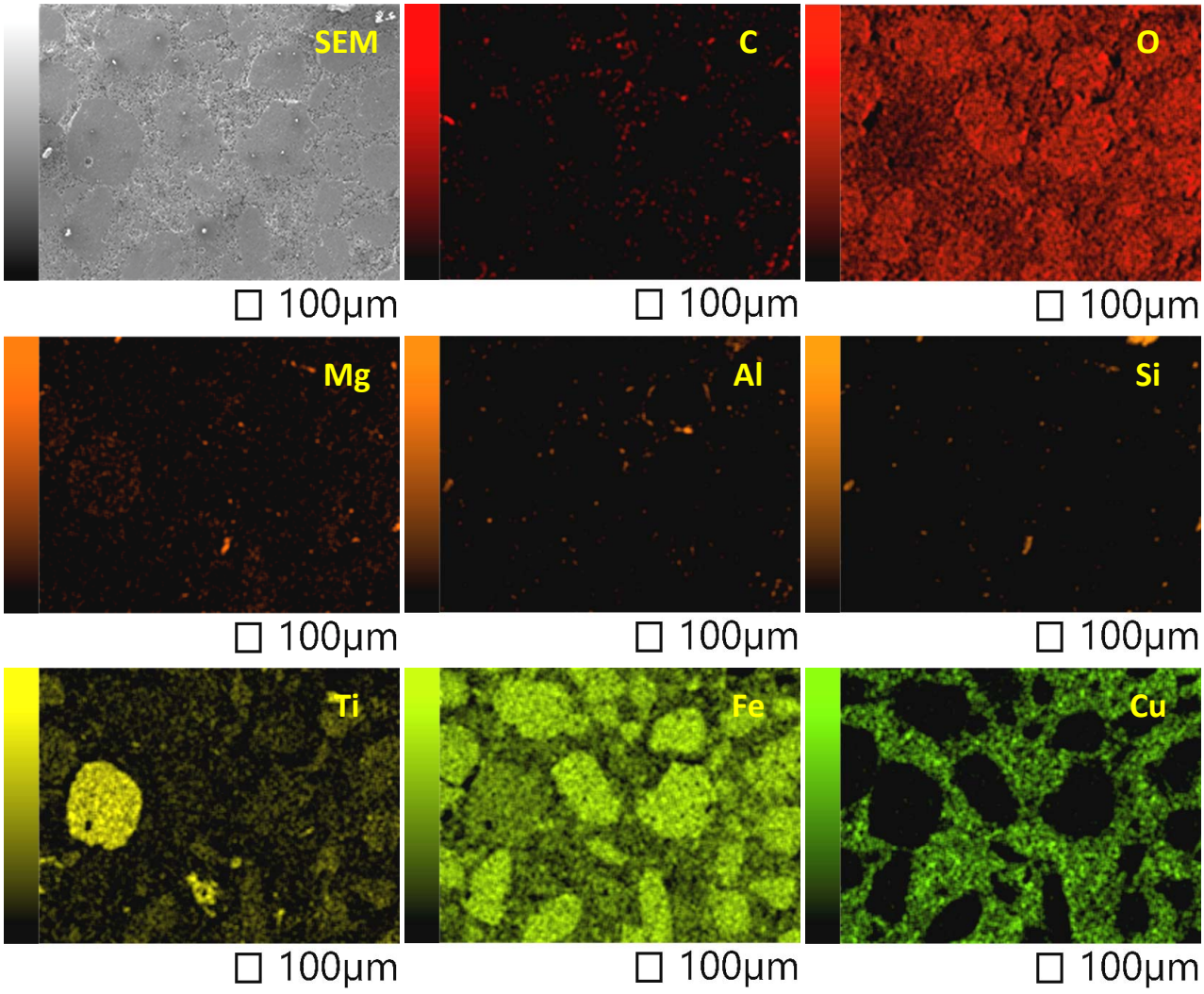

Figure 5. EDS mapping analysis of the Fe-20Cu alloy milled for 16 h and sintered at 800 °C

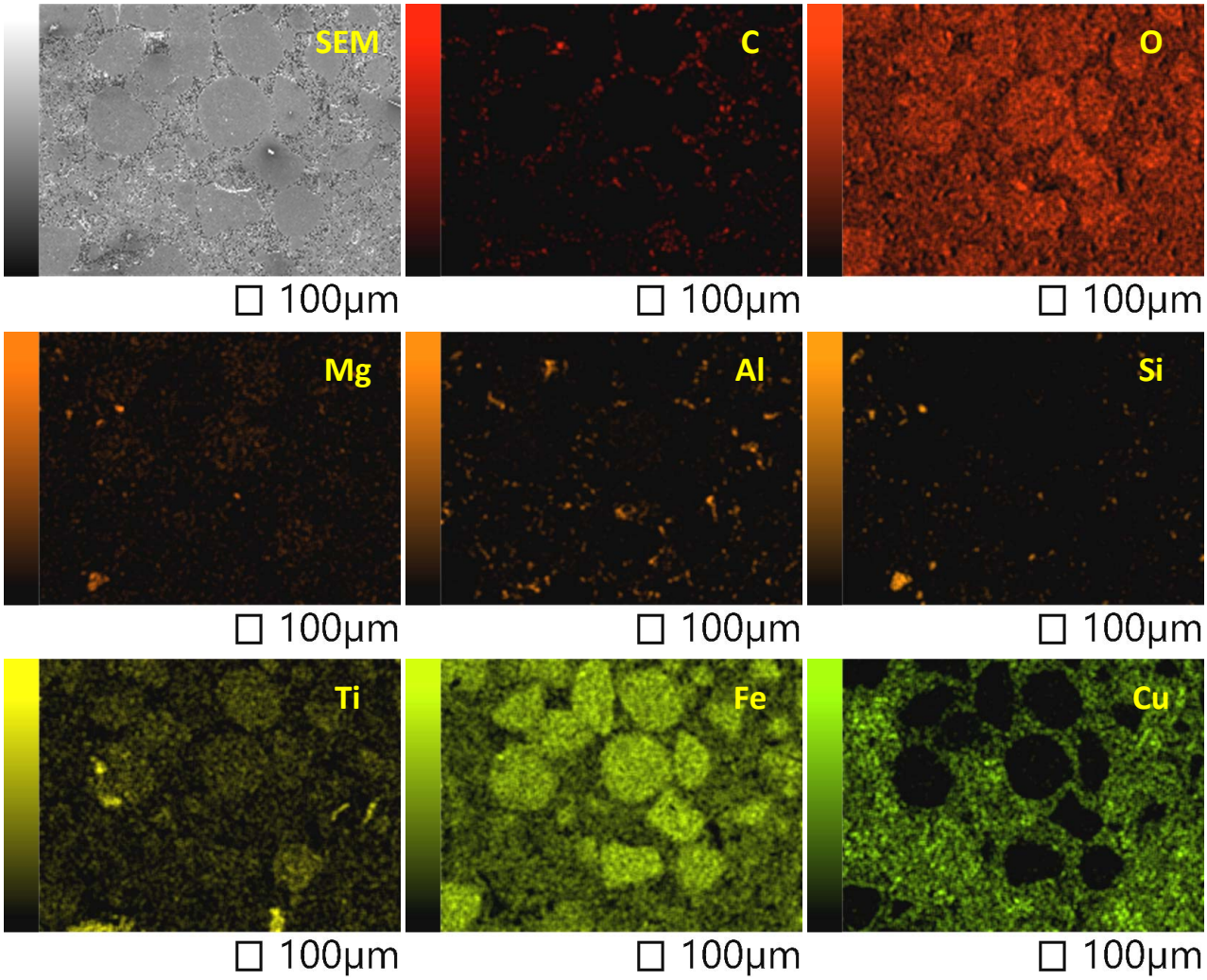

Figure 6. EDS mapping analysis of the Fe-20Cu alloy milled for 16 h and sintered at 900 °C

separation, but the enlarged grain size leads to fewer grain boundaries, which could reduce the obstruction to dislocation motion and thus diminish mechanical strength [27]. Therefore, although sintering at 1000 °C enhances diffusion and structural uniformity, it may adversely affect hardness and strength due to excessive coarsening.

The microstructural changes of powders milled for 16 h and subsequently sintered at 800, 900 and 1000 °C reveal a transition from partial homogenisation to progressive phase separation.

At 800 °C, the alloy shows a refined and relatively uniform distribution, with Fe dispersed throughout the matrix and Cu remaining partially dissolved, with only limited clustering. Moderate oxygen enrichment is noticed along grain boundaries, indicating slight oxidation but without continuous oxide network formation. Minor elements such as Mg, Al, Si and Ti appear sparsely, while localised Ti-rich precipitates act as grain boundary stabilisers, likely restricting grain growth. This condition suggests that sintering at 800 °C facilitates beneficial homogenisation while maintaining opportunities for balanced strength and ductility [28].

At 900 °C, grain coarsening becomes more evident and Fe- and Cu-rich domains are more clearly defined. Cu forms discrete regions embedded within the Fe matrix, while oxygen and minor solute elements, particularly Si and Ti, tend to segregate at grain boundaries, possibly strengthening the grain boundaries. However, they also introduce a potential reduction in ductility due to increased interface brittleness. Therefore, sintering at 900 °C represents an intermediate condition where hardness may be improved, albeit accompanied by a gradual decrease in toughness.

At 1000 °C, the alloy approaches phase equilibrium, consistent with the immiscibility gap in the Fe-Cu system [29]. Cu segregation becomes extensive, forming large clusters or continuous regions, while oxygen accumulates at grain

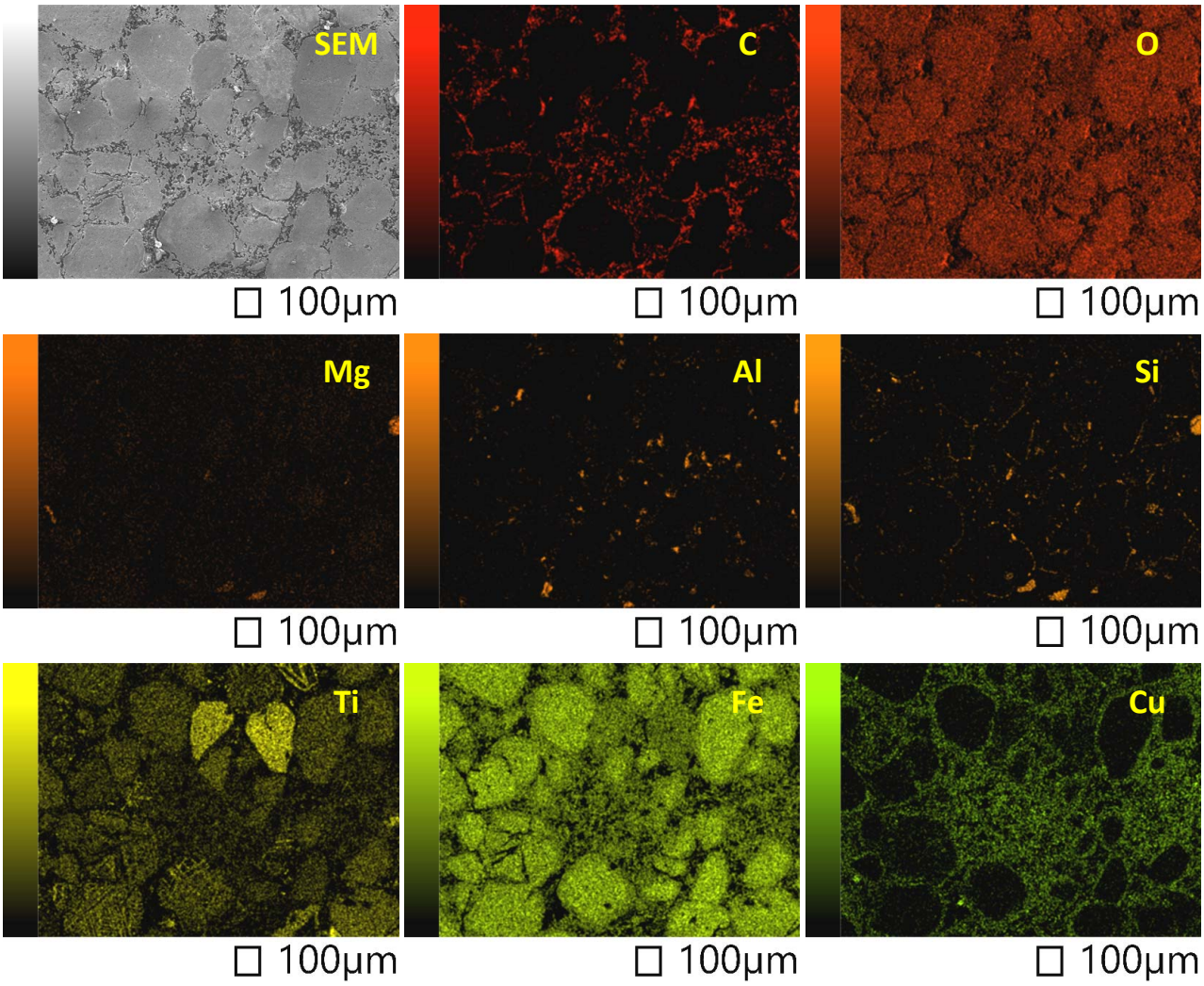

Figure 7. EDS mapping analysis of the Fe-20Cu alloy milled for 16 h and sintered at 1000 °C

boundaries, leading to the formation of more persistent oxide films. Carbon enrichment is also noticed locally, likely associated with carbide stabilisation at boundary sites. Meanwhile, Ti-rich precipitates partially coarsen, diminishing their grain-boundary pinning effect, whereas Si becomes more uniformly distributed along grain interfaces. These features indicate that sintering at 1000 °C promotes diffusion-driven phase separation and secondary precipitation, which may increase hardness through dispersion hardening, yet simultaneously contribute to reduced ductility and fracture resistance.

The EDS maps at 1000 °C reveal pronounced oxygen accumulation along grain boundaries and within Cu-rich areas, suggesting the development of oxide films. This is consistent with the weak Fe_2O_3/CuO-related reflections detected in the XRD patterns of the high-temperature sintered samples [30]. Such grain-boundary oxides locally increase microstructural rigidity but also introduce brittle interfacial sites that can serve as crack-initiation points during sliding, providing a plausible explanation for the slight reduction in wear performance noticed for the most severe sintering conditions.

3.4 Density variation with milling time and sintering temperature

Figure 8 shows that the bulk density of the Fu-Cu alloy systematically increases with prolonged milling and higher sintering temperatures, ranging from 6.04 g/cm^3 in the early-stage milling condition to a maximum of 7.22 g/cm^3 under the most intensive processing schedule. At low-intermediate conditions, densities of 6.04 – 6.58 g/cm^3 indicate incomplete particle bonding and significant residual porosity resulting from insufficient solid-state diffusion. As milling time and thermal energy increase, enhanced interparticle contact and diffusion-driven pore closure yield higher densities in the range of 6.90 – 7.00 g/cm^3.

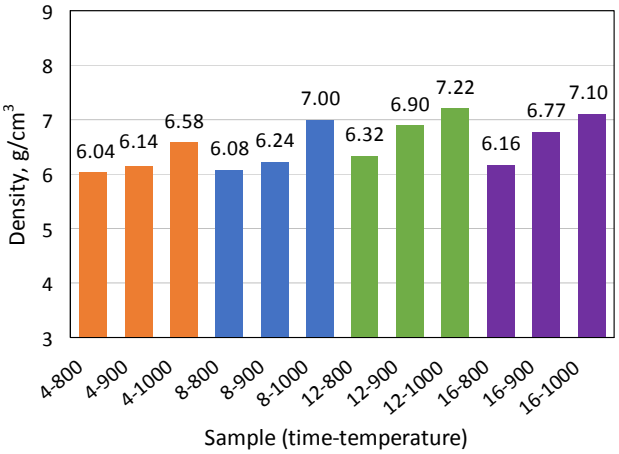

Figure 8. Density for different milling times and sintering temperatures

Peak densification is achieved at the highest combination of milling time and sintering temperature, with measured densities of 7.22 and 7.10 g/cm^3. It should be noted that full densification is not the objective in porous bearing materials, since a moderate and controlled level of porosity is required for lubricant retention. Thus, the improved performance at 12 h milling and 1000 °C reflects an optimal balance between mechanical consolidation and functional pore volume, rather than a pursuit of maximum density. These values reflect improved atomic mobility, grain-boundary migration and neck formation between Fe and Cu particles, which collectively reduce closed porosity and enhance packing efficiency. A slight deviation is noticed for the sample with a density of 6.16 g/cm^3, which may be attributed to excessive sintering, grain coarsening, the formation of surface oxide films or trapped gases that counteract densification despite the elevated temperature.

Overall, the density analysis aligns well with SEM-EDS observations, confirming progressive homogenisation at intermediate processing conditions and partial Fe-Cu segregation or oxide formation at the highest temperatures. Nevertheless, net densification continues to improve once diffusion becomes dominant. The optimal balance between microstructural stability and densification is achieved under long-time milling followed by high-temperature sintering (e.g. 12 h of milling combined with sintering at 1000 °C), approaching the theoretical density predicted by the rule of mixtures. This condition is expected to yield superior mechanical and tribological performance owing to reduced residual porosity and the development of a refined, consolidated microstructure [31].

The highest density obtained (7.22 g/cm^3) represents an increase of approximately 20 %, relative to the lowest density (6.04 g/cm^3), underscoring the pronounced influence of the combined milling and sintering processes on pore closure. Using the measured bulk densities and the theoretical density of Fe-20Cu of approximately 8.1 g/cm^3, the estimated open porosity decreases from roughly 25 % in the least dense samples (6.04 g/cm^3) to about 11 % in the most consolidated ones (7.22 g/cm^3). This trend indicates substantial densification with increasing milling time and sintering temperature, yet a meaningful level of porosity remains. Such residual porosity is essential for porous bearing materials, as it provides lubricant reservoirs that facilitate self-lubrication. Therefore, complete densification is neither targeted nor beneficial for functional performance [32].

3.5 Wear variations with milling time and sintering temperature

Figure 9 illustrates the variation in wear rate of Fe-20Cu alloy as a function of milling time and sintering temperature. The wear rate decreases consistently with longer milling times and increasing sintering temperatures, indicating a strong correlation between microstructural refinement and tribological performance. The highest wear rate of 4.75×10^{-4} mm^3/m is recorded for the sample milled for 4 h and sintered at 800 °C. This relatively poor wear resistance reflects incomplete homogenisation, significant residual porosity and weak interparticle bonding, all of which facilitate material removal under sliding contact.

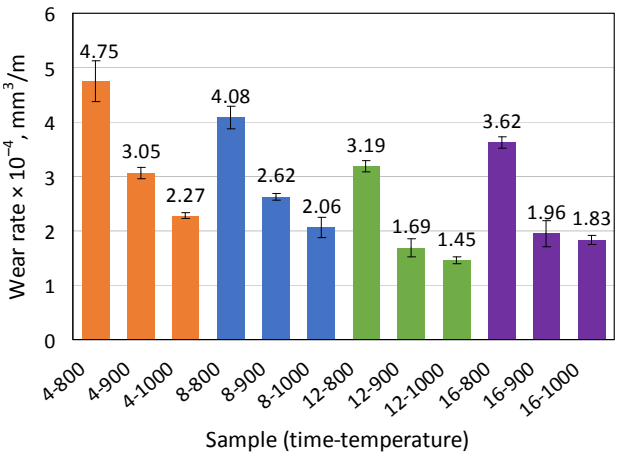

Figure 9. Wear rate for different milling times and sintering temperatures

In contrast, extended milling combined with increased sintering temperature significantly enhances wear resistance. The lowest wear rate of 1.45×10^{-4} mm^3/m is achieved for the sample milled for 12 h and sintered at 1000 °C. This improvement is attributed to enhanced solid-state mixing between Fe and Cu, reduced porosity due to diffusion-assisted densification and the formation of a refined and compact microstructure. These factors collectively improve hardness, structural integrity and resistance to material detachment during loading.

Intermediate processing conditions, such as 8 h of milling and sintering at 900 °C, yield moderate wear performance. Although improved compared with the early-stage samples, these conditions still produce localised coarsening and partial oxide formation, which may serve as weak initiation sites, thereby promoting a delamination-dominated wear mechanism. The noticed wear behaviour therefore reflects the same microstructural trends described earlier, i.e. longer milling and higher sintering temperatures yield improved interdiffusion, reduced porosity and enhanced phase stability, all of which contribute to improved wear resistance.

Overall, the results confirm that extended milling followed by sintering in the 900 – 1000 °C range yields the most favourable tribological response. This outcome correlates strongly with increased material density, microstructural uniformity and phase stabilisation, demonstrating the significant role of diffusion kinetics and defect healing in improving surface durability. Additionally, consistent with the Fe-Cu phase diagram, the immiscibility gap limits homogenisation below approximately 900 °C. Thus, samples sintered at 800 °C exhibit incomplete bonding and substantial open porosity [33].

The SEM micrographs of the wear surface (Fig. 10) further support these findings. The sample milled for 4 h and sintered at 1000 °C exhibits a heterogeneous and severely damaged surface with large pits, grooves and microcracks. At higher magnification, localised detachment, adhesive

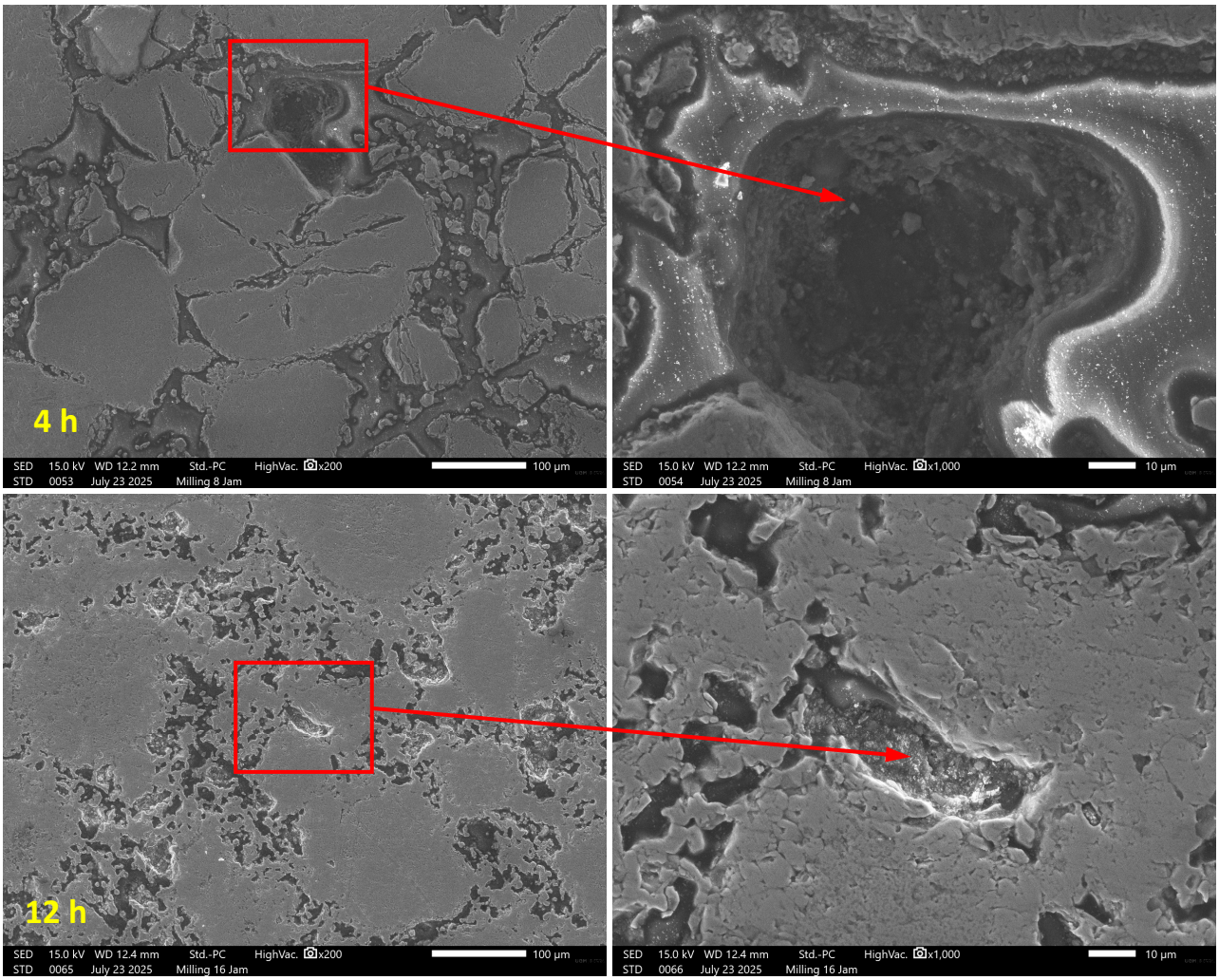

Figure 10. SEM micrograph images of the Fe-20Cu alloy worn surface for specimens milled for 4 and 12 h and sintered at 1000 °C

wear and delamination features are evident. The coexistence of fractured zones and smoother regions confirms microstructural nonhomogeneity due to insufficient milling, where residual porosity facilitates crack initiation and rapid propagation. By comparison, the sample milled for 12 h and sintered at 1000 °C demonstrates a more compact and uniform worn surface. At high magnification, fewer grooves and reduced material removal are noticed. This improvement is attributed to enhanced solid-state mixing, finer crystalline features and better densification achieved through prolonged milling and optimal sintering. Reduced porosity and stronger particle bonding suppress micro-fracturing and delay crack propagation, resulting in lower wear.

The contrast between the samples milled for 4 and 12 h and sintered at 1000 °C emphasises the inherent relationship between porosity, density and wear performance. A porous and weakly bonded microstructure, as seen at shorter milling times, reduced load-bearing capacity and accelerated surface degradation. Conversely, a refined and densified microstructure produced by extended milling improved surface strength and wear resistance. These results demonstrate that precise control of porosity through mechanical alloying and appropriate sintering temperature is essential for approaching theoretical density and achieving superior wear performance in Fe-Cu alloy systems [34]. Although dry sliding tests provide a controlled baseline for evaluating intrinsic wear behaviour, they do not replicate the lubricated and dynamically varying conditions of automotive bearings. Thus, the present result should be interpreted as baseline tribological performance rather than full service-level simulation.

The improvement in wear resistance with increasing milling time and sintering temperature can be rationalised through three dominant microstructural mechanisms. First, extended milling (up to 12 h) refines particle and crystallite size and homogenises Cu dispersion within the Fe matrix, reducing localised plastic deformation. Second, sintering at 900 – 1000 °C promotes neck growth and pore elimination, increasing real contact area. Third, the distribution of Cu governs the wear mode, i.e. finely dispersed Cu domains aid crack blunting and reduce adhesion, whereas over-segregated Cu regions (especially at high temperature) can serve as soft deformation sites, promoting microploughing. Oxygen enrichment noticed along grain boundaries may provide beneficial tribofilm formation or brittle interfaces, depending on its continuity. Together, these effects explain why milling for 12 h and sintering at 1000 °C yield the lowest wear rate by optimising densification, homogenisation and oxide distribution. Quantitatively, the wear rate declined from 4.75×10^{-4} mm^3/m under the 4 h – 800 °C condition to 1.45×10^{-4} mm^3/m for the 12 h – 1000 °C condition, representing an enhancement in wear resistance of approximately 69 %.

4. Conclusions

A Fe-20Cu porous alloy was successfully fabricated by mechanical alloying followed by sintering, with both milling time and sintering temperature exerting a strong influence on microstructural evolution, densification and wear performance.

An optimal processing condition was identified at 12 h of milling combined with sintering at 1000 °C, which produced the highest density (7.22 g/cm^3) and the lowest wear rate (1.45×10^{-4} mm^3/m). The improved tribological behaviour of the sample produced under these conditions is attributed to enhanced Fe-Cu homogeneity, reduced residual porosity and the formation of a refined and well-bonded microstructure, which suppresses severe adhesive and delamination wear mechanisms.

These findings confirm that careful optimisation of mechanical alloying and sintering parameters is essential for achieving high-performance porous Fe-Cu bearing materials suitable for self-lubricating applications.

Acknowledgement

The author would like to express his deepest gratitude to DPPM for providing research funds and international journals, ITNY, BRIN, UNY and the Mechanical Engineering Laboratory of the Faculty of Vocational Studies, UGM Yogyakarta for providing research facilities.

References

[1] E. Şap, Investigation of mechanical properties of Cu/Mo-SiC$_p$ composites produced with P/M, and their wear behaviour with the Taguchi method, Ceramics International, Vol. 47, No. 18, 2021, pp. 25910-25920, DOI: 10.1016/j.ceramint.2021.05.322

[2] D.M. Goudar, J. Haider, K. Raju, R.V. Kurahatti, D.G. Pinto, Influence of Cu addition on the wear behavior of a eutectic Al-12.6Si alloy developed by the spray forming method, Journal of Composites Science, Vol. 8, No. 3, 2024, Paper 88, DOI: 10.3390/jcs8030088

[3] S. Javaid, S. Gupta, Developing sustainable composites for automotive applications, Advanced Materials & Processes, Vol. 180, No. 4, 2022, pp. 14-19, DOI: 10.31399/asm.amp.2022-04.p014

[4] S. Mushtaq, M.F. Wani, Self-lubricating tribological characterization of lead free Fe-Cu based plain bearing material, Jurnal Tribologi, Vol. 12, 2017, pp. 18-37.

[5] S. Şap, Mechanical and tribological behaviour of novel Al-12Si-based hybrid composites, Materials Testing, Vol. 65, No. 4, 2023, pp. 560-577, DOI: 10.1515/mt-2022-0420

[6] Ü. Değirmenci, Mechanical and tribological behavior of a hybrid WC and Al_2O_3 reinforced Al-4Gr composite, Materials Testing, Vol. 65, No. 9, 2023, pp. 1416-1436, DOI: 10.1515/mt-2023-0040

[7] V. Aghaali, T. Ebadzadeh, Z. Karimi, A. Kazemzadeh, E. Marzbanrad, Effect of mechanical alloying and preheating treatment on the phase transformation of the Al-Cu-Fe compacts annealed by microwave radiation, Journal of Materials Research and Technology, Vol. 12, 2021, pp. 749-759, DOI: 10.1016/j.jmrt.2021.02.089

[8] C. Zhang, C. Chen, L. Huang, T. Lu, P. Li, W. Wang, F. Yang, A.A. Volinsky, Z. Guo, Microstructure and properties of Cu-Fe alloys fabricated via powder metallurgy and rolling, Powder Metallurgy, Vol. 64, No. 4, 2021, pp. 308-320, DOI: 10.1080/00325899.2021.1890403

[9] F.M. Lucas, B. Trindade, B.F.O. Costa, G. Le Caër, Mechanical alloying of Fe-Cu alloys from as-received and premilled elemental powder mixtures, Key Engineering Materials, Vol. 230-232, 2002, pp. 631-634, DOI: 10.4028/www.scientific.net/KEM.230-232.631

[10] J.A. Verduzco, A. Molina, R. Guardian, Y.Y. Calderon, S.R. Gonzaga, M. Serrano, H. Villanueva, Synthesis of copper based composites reinforced with $(Ni,Cu)_3Al$ intermetallic via low energy ball milling, Materials Research, Vol. 28, 2025, Paper e20250307, DOI: 10.1590/1980-5373-MR-2025-0307

[11] A. Sun, Y. Liu, D. Wang, Z. Zhou, Sintering behavior and properties of Mo-Cu composites, Advances in Materials Science and Engineering, Vol. 2018, 2018, Paper 8703986, DOI: 10.1155/2018/8703986

[12] M.J. Purnomo, Y.-X. Hsu, I.-S. Yu, C.-Y. Lee, The Effect of Al-5Ti-B addition and applying Helmholtz coils magnetic field for increasing mechanical properties of investment casting A356 Al-Si alloys, International Journal of Metalcasting, Vol. 19, No. 3, 2025, pp. 1788-1802, DOI: 10.1007/s40962-024-01424-3

[13] L. Baroura, A. Boukhobza, A. Derardja, K. Fedaoui, Study of microstructure and mechanical properties of sintered Fe-Cu alloys, International Journal of Engineering Research in Africa, Vol. 34, 2018, pp. 5-12, DOI: 10.4028/www.scientific.net/JERA.34.5

[14] S. Huang, B. Lin, W. Niu, G. Wang, J. Li, Study on the microstructure evolution and mechanical properties of spray-forming Cu-Fe alloys with varying Fe compositions, Journal of Alloys and Compounds, Vol. 1013, 2025, Paper 178452, DOI: 10.1016/j.jallcom.2025.178452

[15] O. Adam, V. Jan, Microstructure evolution of Cu-Fe-based immiscible alloys prepared by powder metallurgy, IOP Conference Series: Materials Science and Engineering, Vol. 1178, 2021, Paper 012001, DOI: 10.1088/1757-899X/1178/1/012001

[16] Ü.A. Usca, S. Şap, M. Uzun, K. Giasin, Evaluation of mechanical and tribological aspect of self-lubricating Cu-6Gr composites reinforced with SiC-WC hybrid particles, Nanomaterials, Vol. 12, No. 13, 2022, Paper 2154, DOI: 10.3390/nano12132154

[17] Ü.A. Usca, S. Şap, M. Uzun, Ü. Değirmenci, Determination of mechanical and tribological properties of vacuum sintered hybrid reinforced Al-4Cu composites, Journal of Composite Materials, Vol. 58, No. 26, 2024, pp. 2799-2815, DOI: 10.1177/00219983241283599

[18] N. Jouini, P. Revel, G. Thoquenne, F. Lefebvre, Characterization of surfaces obtained by precision hard turning of AISI 52100 in relation to RCF life, Procedia Engineering, Vol. 66, 2013, pp. 793-802, DOI: 10.1016/j.proeng.2013.12.133

[19] P.A. Julien, T. Friščić, Methods for monitoring milling reactions and mechanistic studies of mechanochemistry: A primer, Crystal Growth & Design, Vol. 22, No. 9, 2022, pp. 5726-5754, DOI: 10.1021/acs.cgd.2c00587

[20] Z.G. Zheng, Y.B. Chen, J. Wei, X. Wang, Z.G. Qiu, D.C. Zeng, Enhanced M_s of Fe-rich Fe-B-Cu amorphous/nanocrystalline alloys achieved by annealing treatments, Journal of Alloys and Compounds, Vol. 939, 2023, Paper 168621, DOI: 10.1016/j.jallcom.2022.168621

[21] G. Mandal, G. Ma, A. Bandyopadhyay, S. Kunar, A. Sinha, M. Nath, A. Gupta, S. Chabri, Effects of annealing temperature on structure and magnetic properties of mechanically alloyed Cu-Fe-Ti system, Journal of Materials Research and Technology, Vol. 38, 2025, pp. 6126-6133, DOI: 10.1016/j.jmrt.2025.09.076

[22] Z. Huo, G. Zhang, J. Han, J. Wang, S. Ma, H. Wang, A review of the preparation, machining performance, and application of Fe-based amorphous alloys, Processes, Vol. 10, No. 6, 2022, Paper 1203, DOI: 10.3390/pr10061203

[23] M. Mayer, G. Ressel, J. Svoboda, The effect of cryogenic mechanical alloying and milling duration on powder particles' microstructure of an oxide dispersion strengthened FeCrMnNiCo high-entropy alloy, Metallurgical and Materials Transactions A, Vol. 53, No. 2, 2022, pp. 573-584, DOI: 10.1007/s11661-021-06532-x

[24] S. Yang, H. Bao, H. Bai, Y. Li, H. Xu, F. Ma, Effects of Fe solid solute on grain boundaries of bi-crystal Cu: A molecular dynamics simulation, Nano Materials Science, Vol. 6, No. 1, 2024, pp. 86-95, DOI: 10.1016/j.nanoms.2023.05.001

[25] Z. Wang, X. Zhu, C. Wang, X. Xiao, K. Zhang, C. Jiang, J. Liu, Microstructure and mechanical properties of Al/Cu-SS hybrid composite via ball milling and friction stir processing, iScience, Vol. 28, No. 12, 2025, Paper 114008, DOI: 10.1016/j.isci.2025.114008

[26] K. Ming, S. Jiang, X. Niu, B. Li, X. Bi, S. Zheng, High-temperature strength-coercivity balance in a FeCo-based soft magnetic alloy via magnetic nanoprecipitates, Journal of Materials Science & Technology, Vol. 81, 2021, pp. 36-42, DOI: 10.1016/j.jmst.2020.11.057

[27] B.B. Wang, G.M. Xie, L.H. Wu, P. Xue, D.R. Ni, B.L. Xiao, Y.D. Liu, Z.Y. Ma, Grain size effect on tensile deformation behaviors of pure aluminum, Materials Science and Engineering A, Vol. 820, 2021, Paper 141504, DOI: 10.1016/j.msea.2021.141504

[28] S.Y. Peng, Y.Z. Tian, Y. Yang, M. Jiang, H.X. Li, J.W. Wang, S. Li, G.W. Qin, Achieving homogeneous Fe distribution and high strength in Cu-Fe composite consolidated by powder rolling, Materials Science and Engineering A, Vol. 884, 2023, Paper 145563, DOI: 10.1016/j.msea.2023.145563

[29] Q. Chen, R. Chen, J. Su, Q. He, B. Tan, C. Xu, X. Huang, Q. Dai, J. Lu, The mechanisms of grain growth of Mg alloys: A review, Journal of Magnesium and Alloys, Vol. 10, No. 9, 2022, pp. 2384-2397, DOI: 10.1016/j.jma.2022.09.001

[30] S. Ragunath, N. Radhika, A.A. Adediran, Microstructural evolution and wear performance of Ti662 alloy reinforced with FeCoCrCuSi high entropy alloy using microwave sintering, Journal of Materials Research and Technology, Vol. 34, 2025, pp. 2212-2224, DOI: 10.1016/j.jmrt.2024.12.211

[31] L. Miao, H. Wei, J. Yue, R. Chen, Y. Qian, X. Li, Z. Zhu, T. Liu, W. Liao, Superior mechanical properties of a high temperature Co-based superalloy fabricated by laser powder bed fusion, Additive Manufacturing Letters, Vol. 14, 2025, Paper 100311, DOI: 10.1016/j.addlet.2025.100311

[32] J. Sun, K. Yan, Y. Zhu, J. Hong, A high-similarity modeling method for low-porosity porous material and its application in bearing cage self-lubrication simulation, Materials, Vol. 14, No. 18, 2021, Paper 5449, DOI: 10.3390/ma14185449

[33] S. Liu, S. Xu, J. Jie, J. Zhang, Y. Dong, X. Li, T. Li, Microstructure evolution and magnetic properties of metastable immiscible Cu-Fe alloy with micro-alloying B element, Journal of Alloys and Compounds, Vol. 888, 2021, Paper 161627, DOI: 10.1016/j.jallcom.2021.161627

[34] R. Mitra, A. Bajpai, K. Biswas, A critical review on mechanical alloying of high-entropy materials, High Entropy Alloys & Materials, Vol. 3, No. 1, 2025, pp. 1-40, DOI: 10.1007/s44210-025-00056-4